ELSEVIER

Journal of Molecular Catalysis A: Chemical 104 (1995) 95–102

JOURNAL OF MOLECULAR CATALYSIS A: CHEMICAL

Acidity and catalytic properties of $AlPO_4$-11, SAPO-11, MAPO-11, NiAPO-11, MnAPO-11 and MnAPSO-11 molecular sieves

Deepak Bansilal Akolekar

Department of Physical Chemistry, University of New South Wales, P.O. Box No. 1, Kensington, NSW 2033, Australia

Received 1 September 1994; accepted 23 May 1995

Abstract

The type 11 aluminophosphate molecular sieves containing different substituted elements (viz. Mg, Si, Mn, Ni) have been synthesized and characterized for their crystalline nature, N_2-sorption capacity and morphology. Also, the MnAPO-11 molecular sieves with different concentrations of framework-substituted Mn were prepared in order to investigate the changes in the acidity and catalytic properties with the concentration of framework substituted element. The acidity measurements over the aluminophosphate of type 11 catalysts were carried out by the temperature programmed desorption (TPD) and the stepwise thermal desorption (STD) of pyridine using GC techniques. The results of TPD and the STD of pyridine suggests the existence of a broad site energy distribution over these materials. The site energy distribution and the number of strong acid sites are affected by the type of framework substituted element. The magnesium incorporated aluminophosphate of type 11 (MAPO-11) possesses a greater number of strong acid sites than the Mn/Ni/Si-incorporated aluminophosphates of type 11 (MnAPO-11, NiAPO-11, SAPO-11). Among the mono-framework substituted element aluminophosphate molecular sieves, MAPO-11 possesses a greater number of strong acid sites. In the bi-framework substituted element aluminophosphate molecular sieves (MnAPSO-11), the observed strong acid sites are higher in number than the mono-framework substituted element aluminophosphate (MnAPO-11). The catalytic activities of these materials in ethanol, n-hexane, cumene and *o*-xylene reactions were studied. MAPO-11 showed higher conversion in these reactions than $AlPO_4$-11, MnAPO-11, NiAPO-11 and SAPO-11 catalysts. The overall higher conversion was observed over MnSAPO-11.

Keywords: Aluminophosphate; AEL topology; Acidity; Molecular sieves; Site energy distribution

1. Introduction

MeAPO-*n* (metal aluminophosphates), SAPO-*n* (silico-aluminophosphates) and MeAPO-*n* (silico-metal aluminophosphates) are new generation molecular sieves [1–3]. The substitution of metal (Me) atoms into some of Al sites [4–6] or the silicon (Si) atoms into some of the P sites [4,7] or both the metal and silicon atoms into some of the Al and the P sites [4] of an aluminophosphate molecular sieve generates framework acidity and consequently affects the catalytic and adsorptive properties [6–11].

The aluminophosphate of type 11 molecular sieve (AEL topology) reported by Flanigen et al. [1,2], has a unique three dimensional structure with orthorhombic symmetry [12] and cell constants $a = 0.84$ nm, $b = 1.85$ nm and $c = 1.35$ nm. This material is characterized by a 1-dimensional system of channels parallel to *c*-axis with elliptical 10 membered ring and pore dimensions of 0.39 nm $\times$ 0.63 nm. The catalytic properties of the alu-

SSDI 1381-1169(95)00110-7

minophosphate molecular sieves are related to the type and the strength of acid sites. Subsequently, the nature, the strength and distribution of acid sites on the aluminophosphate molecular sieves are dependent on the type of substituted element(s) in the $AlPO_4$-11 framework. Therefore, the present study deals with the acidity/site energy distribution and with the catalytic properties of different T-atom substituted $AlPO_4$-11 type molecular sieves.

2. Experimental

2.1. Molecular sieve preparation

The composition of the gels used for the preparation of type 11 aluminophosphate molecular sieves are presented in Table 1. The procedures followed for the formation of gel and crystallization are already reported [13]. The crystalline material was obtained by the hydrothermal crystallization of the gel initially at 363 K for 24 h and further at 473 K for 24 h in an teflon coated autoclave at autogenous pressure (without agitation). The crystals of the aluminophosphate materials were thoroughly washed with deionized water, filtered, and dried in an air oven at 373 K for 16 h. The organic template was removed by calcination in the presence of air (flow rate 100 $cm^3 \cdot min^{-1}$) at 763 K for 14 h. The sources of

Table 1
Molar oxide ratios in the preparation of aluminophosphate of type 11 catalysts

Catalyst	n-Pr_2NH	MnO_2	NiO	MgO	SiO_2	Al_2O_3	P_2O_5	H_2O
$AlPO_4$-11	1.0	–	–	–	–	1.00	1.00	40
MnAPO-11[A]	1.0	0.04	–	–	–	0.98	1.00	40
MnAPO-11[B]	1.0	0.08	–	–	–	0.96	1.00	40
MnAPO-11[C]	1.0	0.12	–	–	–	0.94	1.00	40
SAPO-11	1.1	–	–	–	0.12	1.00	0.94	40
NiAPO-11	1.0	–	0.12	–	–	0.94	1.00	40
MAPO-11	1.0	–	–	0.12	–	0.94	1.00	40
MnAPSO-11	1.1	0.12	–	–	0.12	0.94	0.94	40

MnO_2, NiO, SiO_2, Al_2O_3 and P_2O_5 were manganese acetate tetrahydrate (Aldrich 99.99%), nickel nitrate hexahydrate (Aldrich, 99.99%), magnesium acetate tetrahydrate (Aldrich, 99.99%), Kieselgel 500 (Merck, FRG), pseudoboehmite (Condea Chemie, FRG) and orthophosphoric acid [85%, Aldrich], respectively. The n-dipropylamine (purity 99%) was supplied by Aldrich.

MnAPO-11[A], MnAPO-11[B] and MnAPO-11[C] samples contains different concentration of framework substituted Mn. The concentration of framework substituted Mn is lowest, intermediate and highest in the MnAPO-11[A], MnAPO-11[B] and MnAPO-11[C], respectively. MnAPO-11[C], NiAPO-11, SAPO-11 and MAPO-11 samples were prepared with similar concentration of substituted element (Mn/Si/Ni/Mg) in the aluminophosphate frameworks for comparing their acidic and catalytic properties. In order to investigate the acidity and catalytic properties of multielement substituted $AlPO_4$-11, MnAPSO-11 containing similar concentration of Mn and Si elements relative to those in MnAPO-11[C] and SAPO-11, respectively, was prepared.

2.2. Molecular sieve characterization

The crystallinity of the products was determined by X-ray diffraction. The atomic absorption spectroscopy and gravimetric analysis were used for the elemental analysis. The size and morphology of the aluminophosphates of type 11 crystals were studied using a JEOL JSM-840A scanning electron microscope. The N_2-sorption capacities of the materials were obtained by N_2-dynamic adsorption technique ($p/p = 0.3$) using a Quantasorb unit (Quantachrome Corp., USA).

2.3. Acidity measurements

The chemisorption of pyridine on the aluminophosphates at 673 K was measured by the GC pulse technique [14] based on temperature-programmed desorption under chromatographic con-

ditions. The STD of pyridine was carried out by desorbing the pyridine chemisorbed at 323 K on the aluminophosphate in a flow of helium from 323 to 673 K in five steps. The temperature in each step was raised at a linear heating rate of 5 $K \cdot min^{-1}$. After the maximum temperature of the respective step was attained, it was maintained for a period of 1 h to desorb the reversibly adsorbed base on the aluminophosphate at that temperature. Details of the procedure for the STD experiments are given elsewhere [15].

2.4. Catalytic activity measurements

The catalytic activity of the catalysts in ethanol, n-hexane, *o*-xylene and cumene reactions have been determined in a pulse microreactor (i.d. 4 mm) connected to a gas chromatograph. The reaction conditions are mentioned in Tables 3–5. Before the activity was measured, the catalyst was heated at 673 K for 1 h in a flow of helium. The details of the microreactor, the experimental procedures for measuring the catalytic activity of the catalysts have been reported earlier [16].

3. Results and discussion

3.1. Characterization

The XRD pattern of the as-synthesized MAPO-11 is shown in Fig. 1. For the other metal substituted aluminophosphates of type 11, the XRD patterns were similar to that of the MAPO-11. The characteristics of the aluminophosphate of type 11 catalysts are presented in Table 1. The crystallinity (obtained from XRD data) and the N_2-sorption capacity measurements indicated high crystallinity for the catalysts. The elemental analysis of the products suggests that the metal (Mn/Ni/Mg) substitutes for some of the Al sites and the Si substitutes for some of the P sites in the aluminophosphate framework. In the metal aluminophosphate, silico-aluminophosphate and silico-metal aluminophosphate frameworks, the metal bonds to phosphorus via oxygen and silicon bonds aluminium viz. oxygen such as –O–P–O–Me–O–P–O–, –O–Si–O–Al–O– and –O–P–O–Al–O–Si–O–Al–O–, respectively. Fig. 2 shows the scanning electron photomicrograph of n-Pr_2NH–$AlPO_4$-11. SEM studies of the materials revealed the presence of similar type of morphology. The crystals of the aluminophosphate of type 11 materials are rectangular in shape and 1.5×2.5 μm in size.

3.2. Acidity/site energy distribution

The site energy distribution obtained from STD of pyridine on $AlPO_4$-11, MnAPO-11[C], NiAPO-11, SAPO-11, MAPO-11 and MnAPSO-

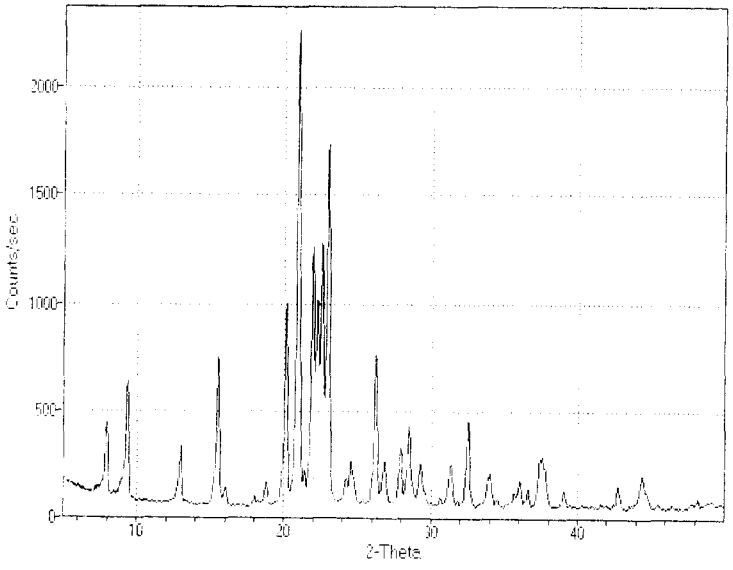

Fig. 1. X-ray powder pattern of Pr_2NH–MAPO-11.

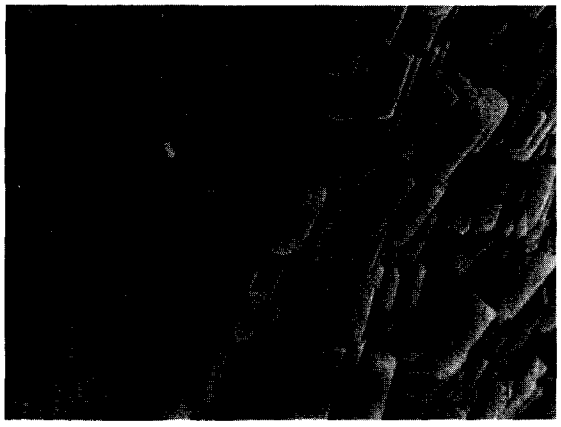

Fig. 2. Typical scanning electron photomicrograph of the aluminophosphate of type 11 (n-Pr_2NH–$AlPO_4$-11) catalyst.

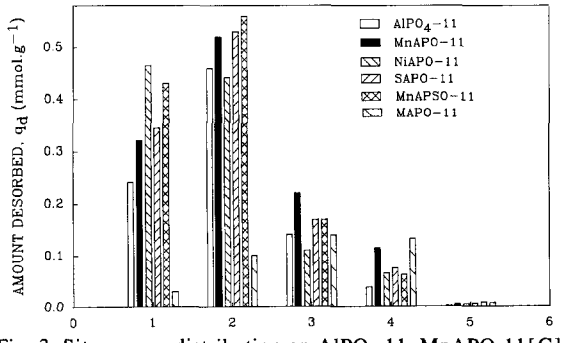

Fig. 3. Site energy distribution on $AlPO_4$-11, MnAPO-11[C], NiAPO-11, SAPO-11, MAPO-11 and MnAPSO-11. 1: 323 < T_d < 373 K; 2: 373 < T_d 473 K; 3: 473 < T_d < 573 K; 4: 573 < T_d < 673 K; 5: 673 < T_d < T_d^*.

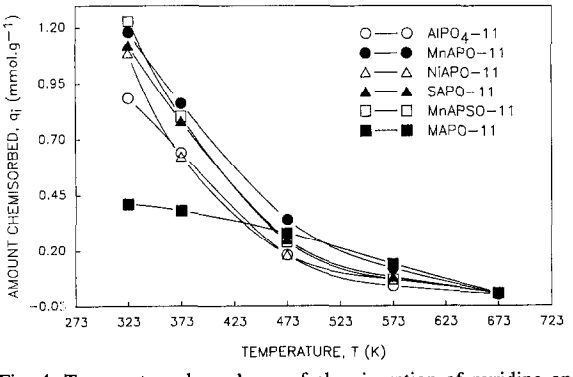

Fig. 4. Temperature dependence of chemisorption of pyridine on $AlPO_4$-11, MnAPO-11[C], NiAPO-11, SAPO-11, MAPO-11 and MnAPSO-11.

11 are shown in Fig. 3. The acid strength of the site involved in the pyridine chemisorption is expressed in the value of desorption temperature (T_d), which lies in the range of temperature in which the chemisorbed pyridine is desorbed. Here, T_d^* corresponds to the temperature at which the pyridine chemisorbed on the strongest sites is desorbed. The columns in the figure show the strength distribution of the sites (equivalent to 0.88 mmol·g^{-1} {for AlPO-11}. 1.98 mmol·g^{-1} {for MnAPO-11 [C]}, 1.09 mmol·g^{-1} {for NiAPO-11}, 1.12 mmol·g^{-1} {for SAPO-11}, 0.41 mmol·g^{-1} {for MAPO-11} and 1.23 mmol·g^{-1} {for MnAPSO-11} involved in the chemisorption at the lowest temperature of the STD (i.e., 323 K). The sites of strength 673 K < T_d < T_d^* were obtained from the amount of pyridine chemisorbed at 673 K. On the other hand, the number of sites of strength $T_1 < T_d < T_2$ were obtained from the amount of pyridine which was initially chemisorbed at T_1 but desorbed by increasing the temperature to T_2. Fig. 4 shows the temperature dependence of the chemisorption of pyridine on $AlPO_4$-11, MnAPO-11[C], NiAPO-11, SAPO-11, MAPO-11 and MnAPSO-11 obtained from the STD data. The chemisorption of pyridine at higher temperatures points to the involvement of the stronger acid sites. The q_i vs. T curve, therefore, presents a type of site energy distribution in which the number of sites are expressed in terms of the amount of pyridine chemisorbed as a function of the temperature. The TPD and the STD of pyridine results have clearly shown that a broad site energy distribution exists on the different element substituted type 11 aluminophosphates. The site energy distribution over the MnAPO-11[C], NiAPO-11, SAPO-11, MAPO-11 and MnAPSO-11 are different. The

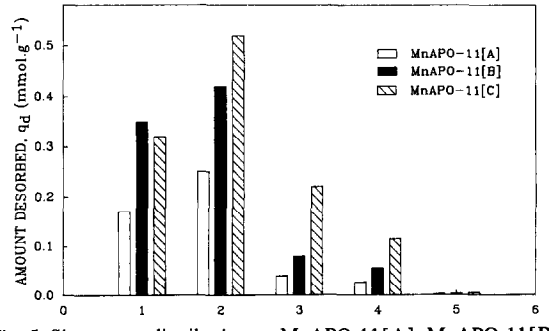

Fig. 5. Site energy distribution on MnAPO-11[A], MnAPO-11[B] and MnAPO-11[C]. 1: 323 < T_d < 373 K; 2: 373 < T_d 473 K; 3: 473 < T_d < 573 K; 4: 573 < T_d < 673 K; 5: 673 < T_d < T_d^*.

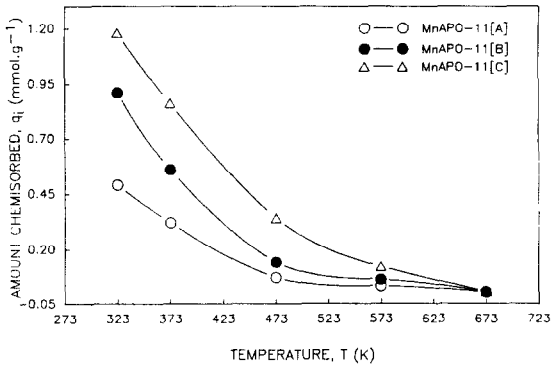

Fig. 6. Temperature dependence of chemisorption of pyridine on MnAPO-11[A], MnAPO-11[B] and MnAPO 11[C].

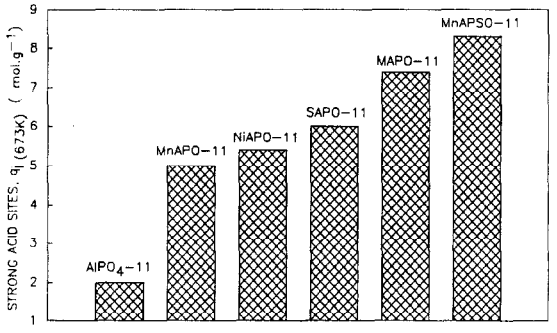

Fig. 7. The number of strong acid sites on $AlPO_4$-11, MnAPO-11[C], NiAPO-11, SAPO-11, MAPO-11 and MnAPSO-11.

weak and the strong acid sites distribution are affected by the element present in the $AlPO_4$-11 framework. MnAPO-11[C], NiAPO-11, SAPO-11 and MnAPSO-11 possesses higher number of weak acid sites than MAPO-11. Fig. 5 and Fig. 6 show the acid strength distribution and the temperature dependence of the chemisorption of pyridine on MnAPO-11[A], MnAPO-11[B] and MnAPO-11[C], respectively. The results indicate that the distribution of weak and strong acid sites are also affected by the Mn content in the $AlPO_4$-11 framework. MnAPO-11[C] (containing higher amount of Mn) possesses a greater number of weak and strong acid sites than MnAPO-11[A] and MnAPO-11[B].

3.3. Strong acid sites

The number of strong acid sites (measured in terms of pyridine chemisorbed at 673 K) (Fig. 7) of the aluminophosphate catalysts are strongly dependent on the element substituted in the $AlPO_4$-11 framework. $AlPO_4$-11 contains a lower number of strong acid sites than the other aluminophosphate catalysts. In the case of the mono-element substituted aluminophosphates, MAPO-11 possesses a higher number of strong acid sites than MnAPO-11[C], NiAPO-11 and SAPO-11. In our earlier investigation [17], it was also observed that the magnesium containing aluminophosphate of type 5 possesses more strong acid sites than SAPO-5 and $AlPO_4$-5. In the multielement substituted aluminophosphate, the combined effect of the two substituted elements on the strong acid sites can be seen in MnAPSO-11. The strong acid sites over MnAPSO-11 are more than the mono element substituted $AlPO_4$-11 materials {viz. MnAPO-11[C], SAPO-11, NiAPO-11, MAPO-11} which is consistent with the values of the framework charge (Table 2). The framework charge on MnAPSO-11 is lower than the other material. Current investigation has revealed that the framework charge and the number of strong acid sites are correlated. The order of the strong

Table 2
Characteristics of the aluminophosphate of type 11 catalysts

Catalyst	Elemental composition	N_2-sorption capacity (mmol $\cdot$ g^{-1})	Framework charge (electron/T atom)
$AlPO_4$-11	(0.50 Al $\cdot$ 0.50 P) O_2	3.53	0.0
MnAPO-11[A]	(0.011 Mn $\cdot$ 0.49 Al $\cdot$ 0.50 P) O_2	3.54	−0.012
MnAPO-11[B]	(0.02 Mn $\cdot$ 0.481 Al $\cdot$ 0.501 P) O_2	3.52	−0.02
MnAPO-11[C]	(0.03 Mn $\cdot$ 0.47 Al $\cdot$ 0.501 P) O_2	3.49	−0.029
SAPO-11	(0.029 Si $\cdot$ 0.501 Al $\cdot$ 0.471 P) O_2	3.47	−0.030
NiAPO-11	(0.031 Ni $\cdot$ 0.469 Al $\cdot$ 0.501 P) O_2	3.51	−0.031
MAPO-11	(0.031 Mg $\cdot$ 0.471 Al $\cdot$ 0.500 P) O_2	3.46	−0.032
MnAPSO-11	(0.029 Mn $\cdot$ 0.03 Si $\cdot$ 0.472 Al $\cdot$ 0.470 P) O_2	3.50	−0.06

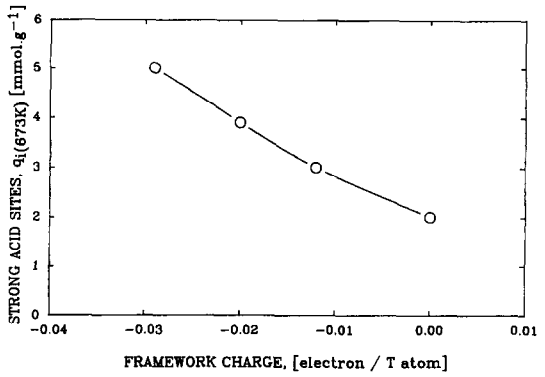

Fig. 8. Correlation between the strong acid sites and the framework charge on $AlPO_4$-11, MnAPO-11[A], MnAPO-11[B] and MnAPO 11[C] catalysts.

acid sites over the materials is as follows: MnAPSO-11 > MAPO-11 > SAPO-11 > NiAPO-11 > MnAPO-11[C]. Correlation between the acidity (strong acid sites measured in terms of the pyridine chemisorbed at 673 K) and the framework charge (obtained from the elemental composition) of the manganese aluminophosphate catalysts is presented in Fig. 8. From the correlation, it is concluded that the number of strong acid sites is increased with the decrease in the framework charge on the aluminophosphate catalysts. The number of strong acid sites increases with the Mn content on MnAPO-11 catalysts.

3.4. Catalytic properties

The product distribution in ethanol over the type 11 aluminophosphate catalysts are given in Table 3. In the ethanol conversion reaction, MAPO-11 showed higher conversion and concentration of aromatics formation as compared with $AlPO_4$-11 and the other aluminophosphate catalysts containing similar concentration of substituted element (MnAPO-11[C], NiAPO-11, SAPO-11). The higher activity and aromatics selectivity exhibited by the MAPO-11 is due to the presence of more strong acid sites. Comparing the results of multielement substituted aluminophosphate (MnAPSO-11) with those of mono element substituted aluminophosphates in ethanol conversion reaction, it is observed that the catalytic activity of MnAPSO-11 is higher than the other materials but the aromatics selectivity is lower than MAPO-11. The observed lower aromatics selectivity over MnAPSO-11 than MAPO-11 is attributed to the presence of higher number selectivity over MnAPSO-11 than MAPO-11 is attributed to the presence of higher number of weak acid sites. The results of ethanol conversion (Table 3) over the MnAPO-11[A], MnAPO-11[B] and MnAPO-11[C] indicated that the catalytic activity and selectivity of aromatics increases with the Mn-content in the $AlPO_4$-11 framework. Current acidity investigations revealed that the number of strong acid sites increases with the Mn-content in the $AlPO_4$-11 framework. The distribution of aliphatics in ethanol conversion reaction is different among the aluminophosphate type 11 catalysts. MAPO-11

Table 3
Conversion of ethanol over the aluminophosphate of type 11 catalysts at 673 K

Catalyst	$AlPO_4$-11	MnAPO-11[A]	MnAPO-11[B]	MnAPO-11[C]	NiAPO-11	SAPO-11	MAPO-11	MnAPSO-11
Conversion (%)	35.4	43.3	51.1	60.1	64.5	71.3	81.5	88.5
Aromatics conc. (wt%)	0.6	0.9	1.1	1.6	1.8	2.2	3.1	2.8
Product distribution (wt%)								
CH_4	–	–	–	–	–	–	0.1	–
C_2-aliphatics	90.4	87.8	85.7	81.1	83.9	80.6	79.1	81.3
C_3-aliphatics	4.1	5.0	6.0	7.9	7.6	9.1	8.0	8.2
C_4-aliphatics	2.6	2.8	3.4	4.9	3.1	4.2	5.1	3.8
C_{5+}-aliphatics	1.2	2.3	2.7	3.7	2.6	3.0	3.9	3.4
Aromatics	1.7	2.1	2.2	2.7	2.8	3.1	3.8	3.3
Total	100	100	100	100	100	100	100	100

Reaction conditions: Amount of catalyst 0.28 g, He flow rate 60 $cm^3 \cdot min^{-1}$, pulse size 3 μl.

Table 4
The catalytic activities of the aluminophosphate of type 11 catalysts in n-hexane and cumene cracking reactions at 673 K

Catalyst	n-Hexane conversion (%) [a]	Cumene conversion (%) [b]
$AlPO_4$-11	1.1	8.1
MnAPO-11[A]	2.4	9.2
MnAPO-11[B]	3.5	11.1
MnAPO-11[C]	4.6	16.5
NiAPO-11	4.5	18.0
SAPO-11	5.8	26.4
MAPO-11	7.1	43.3
MnAPSO-11	7.8	36.5

[a] Reaction conditions: amount of catalyst 0.30 g; He flow rate 30 $cm^3 \cdot min^{-1}$; pulse size 1 μl.
[b] Reaction conditions: amount of catalyst 0.1 g; He flow rate 30 $cm^3 \cdot min^{-1}$; pulse size 1 μl.

showed the lower C_2-aliphatics formation and the higher C_4- and C_{5+}-aliphatics and aromatics formation as compared to the other catalysts. The C_2-aliphatics formation decreases and the formation of C_3-, C_4- and C_{5+}-aliphatics and aromatics increases with the Mn content in the MnAPO-11 catalyst.

The catalytic activities of the aluminophosphate catalysts in the n-hexane and cumene cracking reactions at 673 K are presented in Table 4. The results indicate that the catalytic activities of the catalysts in these reactions differs with the type and the concentrations of the element substituted in the aluminophosphate framework. In the n-hexane conversion reaction, MnAPSO-11 shows higher conversion and the catalytic activity order of the is same as those of strong acid sites. The order of aromatics formation in n-hexane conversion over the catalysts is as follows: MAPO-11 (2.4 wt%) > MnAPSO-11 (2.0 wt%) > SAPO-11 (1.6 wt%) > NiAPO-11 (1.0 wt%) > MnAPO-11[C] (0.9 wt%) > MnAPO-11[B] (0.5 wt%) > MnAPO-11[A] (0.3 wt%) > $AlPO_4$-11 (0.2 wt%). The cracking of cumene was highest over MAPO-11.

In isomerization of *o*-xylene (Table 5), MAPO-11 showed higher catalytic activity and formation of more toluene and C_{9+}-aromatics as compared with MnAPO-11[C], NiAPO-11 and SAPO-11. MAPO-11 exhibited lower *p*- and *m*-xylenes selectivity and the higher xylene loss among the catalysts. The results of *o*-xylene isomerization over the manganese aluminophosphate catalysts indicated the increase in the *o*-xylene conversion and the xylene loss with the concentration of Mn in the aluminophosphate catalysts. The observed higher conversion of *o*-xylene over MnAPSO-11 is consistent with the presence of stronger acid sites among the other type 11 aluminophosphate catalysts.

Table 5
Isomerization of *o*-xylene over the aluminophosphate of type 11 catalysts at 673 K

Catalyst	$AlPO_4$-11	MnAPO-11[A]	MnAPO-11[B]	MnAPO-11[C]	NiAPO-11	SAPO-11	MAPO-11	MnAPSO-11
Conversion (%)	4.6	6.8	9.1	13.1	13.8	15.3	18.9	20.7
Product distribution [hydrocarbon (wt%)]								
Aliphatics	0.1	0.2	0.2	0.3	0.3	0.4	0.3	0.3
Benzene	0.1	0.3	0.4	0.4	0.6	0.4	0.5	0.6
Toluene	0.2	0.6	0.9	1.3	2.2	2.0	3.1	2.6
p-Xylene	1.6	2.3	3.1	4.6	4.8	5.6	6.1	6.8
m-Xylene	2.4	3.0	3.9	5.8	5.4	6.4	7.9	8.9
o-Xylene	95.4	93.2	90.9	86.9	86.2	84.7	81.1	79.6
C_{9+}-aromatics	0.2	0.4	0.6	0.7	0.5	0.9	1.5	1.2
Total	100	100	100	100	100	100	100	100
Xylene loss (wt%)	0.6	1.5	2.1	2.7	3.6	3.3	4.9	4.7
p-X/*m*-X	0.67	0.77	0.79	0.79	0.89	0.88	0.77	0.76
Selectivity for *p*- and *m*-xylenes	87.0	78.0	77.0	79.4	75.3	78.4	74.0	77.0

Reaction conditions: amount of catalyst 0.35 g; He flow rate 30 $cm^3 \cdot min^{-1}$; pulse size 1 μl.

4. Conclusions

The studies on the acidic and catalytic properties of different element substituted aluminophosphate of structure type 11 catalysts leads to the conclusions that the acidity, site energy distribution, the number of strong acid sites and the catalytic activities of these materials are strongly dependent on the nature and concentration of element substituted in the $AlPO_4$-11 framework. The acidity and activity of the type 11 aluminophosphate catalyst are also affected by the presence of more than one substituted element.

Acknowledgements

The author is grateful to the Alexander von Humblodt Foundation, Bonn, Germany for an award of an international research fellowship.

References

[1] E.M. Flanigen, B.M. Lok, R.L. Patton and S.T. Wilson, Stud. Surf. Sci. Catal., 28 (1986) 103.
[2] E.M. Flanigen, B.M. Lok, R.L. Patton and S.T. Wilson, Pure Appl. Chem., 58 (10) (1986) 1351.
[3] B.M. Lok, C.A. Messina, R.L. Patton, R.T. Gajek, R.T. Cannan and E.M. Flanigen, J. Am. Chem. Soc., 104 (1984) 1146.
[4] E.M. Flanigen, R.L. Patton and S.T. Wilson, Stud. Surf. Sci. Catal., 37 (1988) 13.
[5] D.B. Akolekar, J. Catal., 143 (1993) 227.
[6] D.B. Akolekar and S. Kaliaguine, J. Chem. Soc., Faraday Trans., 89 (22), (1994) 4141.
[7] D.S. Dzwigaj, M. Briend, A. Shikholesami, M.J. Peltre and D. Barthomeuf, Zeolites, 10 (1990) 157.
[8] E.M. Flanigen and S.T. Wilson, ACS Symp. Ser., 398 (1989) 329.
[9] K.-H. Schnabel, R. Fricke, I. Girnus, E. Jahn, B. Loffler, B. Parlitz and C. Peuker, J. Chem. Soc. Faraday Trans., 87 (21) (1991) 3569.
[10] C. Bezouhabova, Y. Kalvachev and H. Lechert, J. Chem. Soc., Faraday Trans., 87 (19) (1991) 3315.
[11] A.F. Ojo, J. Dwyer, J. Dewing, J.P. O'Malley and A. Nabhan, J. Chem. Soc., Faraday Trans., 88 (1) (1992) 105.
[12] J.M. Bennett, Jr. Richardson, J.W. Pluth and J.V. Smith, Zeolites, 7 (1987) 160.
[13] N.J. Tapp, N.B. Milestone and D.M. Bibby, Zeolites, 8 (1982) 183.
[14] V.R. Choudhary and V.S. Nayak, Appl. Catal., 4 (1983) 31.
[15] V.R. Choudhary, J. Chromatogr., 268 (1983) 207.
[16] V.S. Nayak and V.R. Choudhary, Appl. Catal. 4 (1982) 333.
[17] D.B. Akolekar, Zeolites, 14 (1994) 53.